Lithium-Sulfur Battery

International Edition: DOI: 10.1002/anie.201708746
German Edition: DOI: 10.1002/ange.201708746

High Sulfur Content Material with Stable Cycling in Lithium-Sulfur Batteries

Molleigh B. Preefer, Bernd Oschmann, Craig J. Hawker, Ram Seshadri,* and Fred Wudl**

Abstract: *We demonstrate a novel crosslinked disulfide system as a cathode material for Li-S cells that is designed with the two criteria of having only a single point of S–S scission and maximizing the ratio of S–S to the electrochemically inactive framework. The material therefore maximizes theoretical capacity while inhibiting the formation of polysulfide intermediates that lead to parasitic shuttle. The material we report contains a 1:1 ratio of S:C with a theoretical capacity of 609 mAh g^{-1}. The cell gains capacity through 100 cycles and has 98% capacity retention thereafter through 200 cycles, demonstrating stable, long-term cycling. Raman spectroscopy confirms the proposed mechanism of disulfide bonds breaking to form a S–Li thiolate species upon discharge and reforming upon charge. Coulombic efficiencies near 100% for every cycle, suggesting the suppression of polysulfide shuttle through the molecular design.*

With increasingly widespread use of renewable energy from intermittent sources such as solar and wind comes a pressing need for improved energy storage devices. However, currently used lithium-ion batteries involve intercalation, specifically layered oxide cathodes with graphite anodes, which limit energy densities and specific capacities due to the relatively heavy host structures and state of charge limitations. One of the most promising systems to overcome this challenge is Li-S batteries,[1] owing to its high theoretical gravimetric capacity based on a conversion redox reaction (1675 mAh g^{-1} assuming reduction of S^0 to S^{2-}), making it especially attractive for applications in portable electronics and electric vehicles. Additionally, sulfur is nontoxic and an under-utilized, abundant byproduct of oil refining, making it a sustainable alternative to toxic, expensive transition metals used in common intercalation materials.[2]

Major challenges of Li-S batteries include the low electronic conductivity of sulfur,[3] leading to low utilization of active material and therefore low capacity. Additionally, volume changes during cycling result in the loss of electrical contact, leading to device failure.[4–6] Furthermore, when sulfur is cycled with commonly used ether-based electrolytes, soluble polysulfide intermediates form[7,8] and create what is known as polysulfide shuttle.[9,10] These soluble intermediates migrate between the anode and the cathode, cause rapid capacity fade and poor Coulombic efficiency, eventually short-circuiting the cell.

There have been many efforts to combat polysulfide shuttle, including nanostructured carbon–sulfur cathodes,[11–14] polysulfide reservoirs,[15,16] encapsulation in carbon[17–23] and TiO_2,[24] polysulfide mediators,[25,26] and altering solvent conditions,[27–30] among others.[31–33] Our approach exploits the chemical functionality of disulfides to prevent the initial formation of polysulfides by only providing one point of electrochemical scission. De Jonghe et al. have shown impressive electrochemical reversibility using disulfide-containing solid-state cathode materials with polyethylene oxide electrolytes versus lithium, however the sulfur content of the active material is a maximum of 33 atom percent or less.[34–36] To address this challenge, we have designed a crosslinked disulfide with 50 atom percent sulfur content (C_6S_6 monomer containing roughly 50 mol% S and 50 mol% C) that operates using the conventional Li-S electrolyte system, bis(trifluoromethane)sulfonamide lithium salt (LiTFSI) in dioxolane (DOL) and dimethoxyethane (DME).

The new, highly stable Li-S cell we report has a theoretical gravimetric capacity of 609 mAh g^{-1} based on 6 moles of lithium per C_6S_6 monomer unit. The high sulfur content benefits the performance two-fold: there is potential for high gravimetric capacity and, if full conversion occurs, creates a highly charged discharged product. In its discharged state, the active material is expected to form $C_6S_6^{6-}$ with six Li^+ counterions, creating a highly charged structure that is insoluble in the ether-based electrolyte. This allows the material to undergo a reversible redox reaction over hundreds of charge cycles without shuttle or capacity fade. Additionally, if full reduction does not occur, the monomer units will be bound in the crosslinked framework, also preventing dissolution into the electrolyte.

The crosslinked disulfide polymer was obtained in a three-step synthesis described in Scheme 1. $C_6(SLi)_6$ was synthe-

[*] M. B. Preefer, Prof. Dr. C. J. Hawker, Prof. Dr. R. Seshadri
Department of Chemistry and Biochemistry, University of California
Santa Barbara, CA 93106 (USA)
M. B. Preefer, Dr. B. Oschmann, Prof. Dr. C. J. Hawker,
Prof. Dr. R. Seshadri
Materials Research Laboratory, University of California
Santa Barbara, CA 93106 (USA)
E-mail: hawker@mrl.ucsb.edu
seshadri@mrl.ucsb.edu
Prof. Dr. C. J. Hawker, Prof. Dr. R. Seshadri, Prof. Dr. F. Wudl
Materials Department, University of California
Santa Barbara, CA 93106 (USA)
E-mail: wudl@chem.ucsb.edu
M. B. Preefer, Dr. B. Oschmann, Prof. Dr. C. J. Hawker,
Prof. Dr. R. Seshadri, Prof. Dr. F. Wudl
Mitsubishi Chemical Center for Advanced Materials, University of California
Santa Barbara, CA 93106 (USA)
Supporting information and the ORCID identification number(s) for the author(s) of this article can be found under https://doi.org/10.1002/anie.201708746.

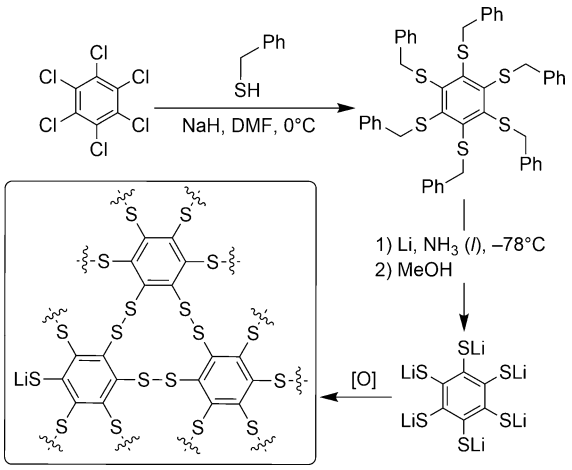

Scheme 1. Synthesis scheme of crosslinked disulfide active material.

sized from a modified procedure previously reported by Harnisch and Angelici,[37] which was subsequently oxidized in purified air to obtain the crosslinked structure. The thiol form of the intermediate structure, benzenehexathiol (BHT), is well-studied and is commonly used as a ligand in MOF and coordination polymer chemistry.[38,39] Lithium was used as the counterion in the thiolate intermediate so that the starting material would be assembled in a partially discharged state for an Li-S cell if the material does not fully crosslink at every site.

Solid state ^{13}C NMR with magic angle spinning shows a signal at 127 ppm arising from aromatic C. The presence of a shoulder at 137 ppm (Figure 1a) and a ^{7}Li NMR signal at 0 ppm (Figure S1 in the Supporting Information) suggest the presence of residual thiolate. However, the sulfur high-resolution X-ray photoelectron spectrum (XPS) indicates the presence of only one sulfur oxidation state (Figure 1c), and the lithium high-resolution spectrum shows no signal (Figure 1d). Therefore, the disulfide active material is almost entirely crosslinked prior to cycling.

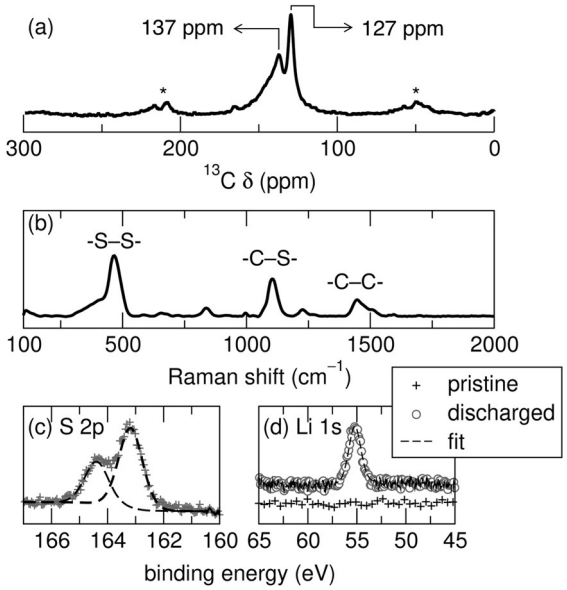

Figure 1. Characterization of the disulfide active material prior to electrochemical testing. a) ^{13}C NMR spectrum with MAS at 16 kHz show two peaks in the aromatic region, and the asterisks label the spinning sidebands. b) Raman spectrum with labelling of characteristic peaks. c) High-resolution XPS in the sulfur 2p region with fits for the $2p^{1/2}$ and $2p^{3/2}$ components of one oxidation state. d) High resolution XPS in the lithium 1s region of the pristine material (no peak detected) and the discharged material at 1.0 V.

Raman spectroscopy (Figure 1b) provides significant structural insight into the materials, both in the pristine state and at different states of charge. The pristine disulfide powder displays a strong disulfide peak at 480 cm^{-1}, assigned from previous literature.[40,41] Also seen is a strong aromatic C–S mode at 1050 cm^{-1}, as well as an aromatic C–C mode at 1450 cm^{-1} (Figure 1b). These three peaks signify the major structural components of the active material, notably benzene rings connected through disulfide bonds.

Electrochemical testing of the disulfide material reflects stable cycling through both cyclic voltammetry (CV) and galvanostatic cycling with potential limitation (GCPL) with lithium as both the anode and the reference electrode. CV was performed in a coin cell at 0.1 mV s^{-1} and indicates reversibility is established after the first cycle (Figure 2a). The main reduction occurs at 2.25 V with a less pronounced reduction at 2.18 V. There is a one-step oxidation at 2.5 V. GCPL also reflects the same redox potentials from the presence of plateaus at the corresponding potentials (Figure 2b). The galvanostatic cycling was performed with

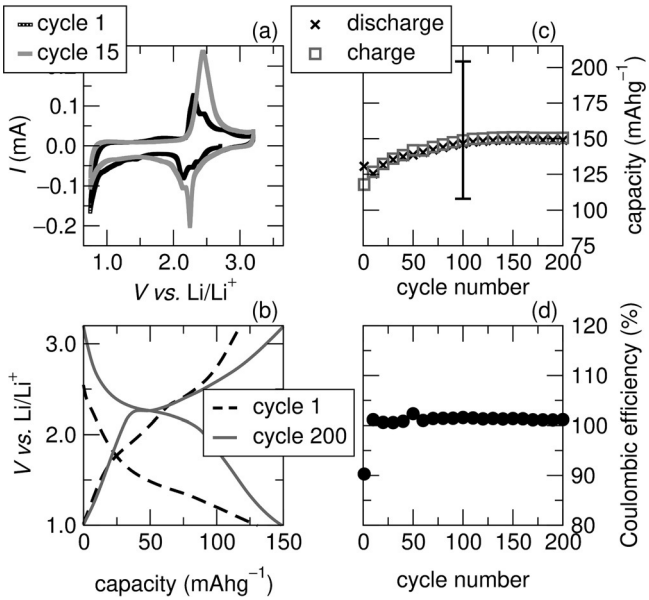

Figure 2. Electrochemistry of the disulfide material with LiTFSI in DOL/DME as the electrolyte system, and Li is both the anode and the reference electrode. a) Cyclic voltammetry from 3.2 V to 0.75 V at a sweep rate of 0.1 mV s^{-1}. b) Galvanostatic cycling with potential limitation (GCPL) at a rate of C/10 from 3.0 V to 1.0 V shown for 200 cycles. c) Capacity for each cycle (charge and discharge) from GCPL increases through cycle 100 and maintains 150 mAh g^{-1} through 200 cycles. The error bar at cycle 100 represents the standard deviation of capacities observed over 10 different cells. d) Coulombic efficiency, defined as charge divided by discharge capacity, hovers around 100% for all 200 cycles.

identical coin cells for 200 cycles. The gravimetric capacity grows over the first 100 cycles and stabilizes through cycle 200 with 98% capacity retention (Figure 2c). The Coulombic efficiency nears 100% for all cycles following cycle 1 (Figure 2d), suggesting the crosslinked disulfide material circumvents one of the most detrimental processes in classical Li-S batteries, parasitic polysulfide shuttle. All electrochemical testing was done without any additives to the electrolyte or the cathode material, demonstrating the exceptional stability of the disulfide material. Extended electrochemical testing is demonstrated with fewer cells to confirm its longevity (Figure S2).

Ex situ analysis provides confirmation for and insight into how the active material performs at the molecular level and microstructural level. Raman spectroscopy is particularly useful for confirming the mechanism by which redox occurs. The disulfide bond, which is the only electrochemically active part of the material, can be tracked by the peak at 480 cm^{-1}, starting in the pristine material. Once cast, the Raman spectrum shows the emergence of the graphitic bands at 1350 cm^{-1} and 1580 cm^{-1} from the Ketjen Black carbon additive (Figure 3a, shaded region). Spectra were taken after 100 cycles at the most charged and discharged states, 3.2 V and 1.0 V, respectively. The charged product clearly shows a strong disulfide peak that even grows in intensity from the pristine material, suggesting an increase in crosslinking. The peak at 480 cm^{-1} recedes in the spectrum of the discharged product, and a new peak at 270 cm^{-1} emerges. By comparison with a less easily oxidized analogous material, lithium benzene-1,3,5-tris(thiolate), the peak at 270 cm^{-1} can be assigned to −S−Li (Figure S3). Therefore, the presence of the disulfide peak for the charged state and its suppression upon discharging indicate the electrochemical cleavage and reformation of the disulfide bonds in the network. A larger sampling of Raman spectra (Figure S4) suggests that complete conversion is not taking place during cycling, which is consistent with the material not reaching theoretical capacity during cycling. Different regions in the electrodes display different extents of charge or discharge, suggesting not all particles undergo redox with every cycle.

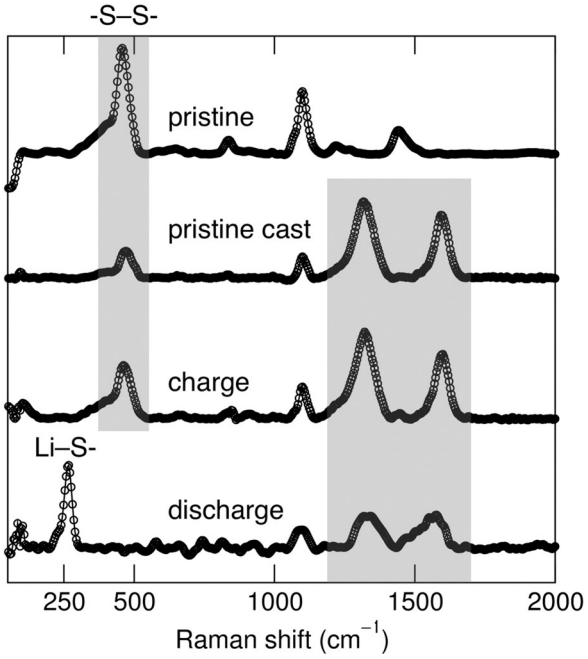

Figure 3. Raman spectroscopy of the pristine powder, pristine electrode, charged, and discharged products compare disulfide bonds breaking and reforming. The highlighted region from 1350 cm^{-1} to 1580 cm^{-1} indicates the graphitic contribution from the Ketjen Black additive.

Scanning electron microscopy (SEM) provides further understanding of the capacity gain over the first 100 cycles, which is an unexpected occurrence in the Li-S system. Comparing SEM images from the cast electrodes before and after cycling reveals the disulfide particles undergo self-microstructuring, creating porosity over many cycles (Figures S5, S6). The increased surface area may account for the capacity gain seen in the galvanostatic cycling over the first 100 cycles, as lithium can access the densely-crosslinked active material more readily at the surface. Once the particles have undergone this microstructural change, the electrochemical performance reaches a steady state, and the capacity does not change from cycle 100 through 200.

In summary, we report a new crosslinked disulfide material that exhibits stable cycling over hundreds of cycles and good Coulombic efficiency with no electrolyte additives and minimal device engineering. The use of a disulfide active material with maximized sulfur content prevents polysulfide shuttle by providing only one point of electrochemical scission, a crosslinked framework, and a highly charged discharged product. With increased optimization, particularly engineering the electrodes to incorporate improved ionic and electronic properties, the cathode material reported herein has potential for practical applications with capacities close to the theoretical amount.

Experimental Section

Preparation and characterization of disulfide active material: Complete characterization of intermediate products can be found in the Supporting Information.

Synthesis of hexakis(benzylthio)benzene: Hexakis(benzylthio)benzene was synthesized by a modified procedure reported by Harnisch and Angelici.[37] NaH (60% dispersion in mineral oil), hexachlorobenzene (analytical grade), benzyl mercaptan (99%), Li chips, and NH_3 were used as received from Sigma Aldrich. All solvents were dried at a solvent system before use. After washing 8.0 g of NaH (60% dispersion in oil, 0.20 mol) with 3 × 20 mL of hexanes and with 2 × 20 mL of DMF, NaH was suspended in 150 mL of DMF and cooled to 0 °C. Benzyl mercaptan (23.5 mL, 0.20 mol) was added slowly to the suspension followed by the addition of hexachlorobenzene (4.76 g, 16.7 mmol). The reaction mixture was stirred for 10 min at 0 °C before it was allowed to warm to room temperature. The mixture was stirred at room temperature overnight. 10 mL of isopropyl alcohol was added to the reaction mixture and stirred for 15 minutes, followed by the addition of 75 mL of deionized water. The mixture was extracted with chloroform and dried with magnesium sulfate. The organic layer was concentrated to 200 mL using reduced pressure, and the product was precipitated with 400 mL of methanol. ^{1}H NMR (500 MHz, CD_2Cl_2): $\delta = 7.22$ (m, 5H, Ar-H), 4.07 ppm (s, 2H, CH_2).^{13}C NMR (500 MHz, CD_2Cl_2): $\delta = 147$, 138, 129, 128, 127, 42 ppm. FDMS TOF m/z: Calcd for $C_{48}H_{42}S_6$ 810.16; Found 810.13.

Synthesis of crosslinked lithium benzene hexathiolate: 496 mg of Li (71 mmol) was added to 70 mL of liquid ammonia at −78 °C. A solution of hexakis(benzylthio)benzene (4.8 g, 6.0 mmol) in 15 mL of dry THF was added. After stirring for one hour at −78 °C, 30 mL of degassed methanol were added and the reaction mixture was warmed to room temperature over 2 hours. 50 mL of degassed water were added and side products were removed by the extraction with diethyl ether. Lithium benzene hexathiolate (1.2 g, 65 % yield) was concentrated by freeze drying. The hexathiolate is extremely air-sensitive, so crosslinking was conducted immediately by dissolving lithium benzene hexathiolate (250 mg, 0.8 mmol) in water (10 mL) and by purging with air purified through a bubbler of sulfuric acid for 48 hours. The crosslinked material precipitated during purging. After 48 hours, the reaction mixture was centrifuged to isolate the precipitated material. The material was redispersed in water and centrifuged followed by two more redispersion and centrifugation steps. The final product was isolated by freeze drying over night with a yield of 180 mg (84 %).

Preparation and characterization of electrodes: The active disulfide material and conductive carbon additive (AzkoNobel Ketjenblack EC-600JD) were mixed in an aqueous dispersion of carboxymethyl cellulose (CMC) and styrene-butadiene rubber (SBR) (CMC:SBR = 1:1 wt/wt) in a weight ratio of disulfide:KB:CMC/SBR = 50:35:15. The slurry was cast on carbon coated aluminium foil as the current collector (Toya-Carbo-50G01, Toyal) and dried at 60 °C for 12 h under vacuum. Disc electrodes with a diameter of 10 mm were punched after drying. Active material mass loadings were in the range of 0.8 mg and 1.2 mg per electrode. Average thickness of the electrodes was 30 μm.

Electrochemical measurements: Galvanostatic cycling was conducted using 2032-type coin cell (MTI Corporation) with metallic Li as the counter electrode. 19 mm disks of polypropylene (Celgard 3501) were used as the separator, and the electrolyte was composed of 1.0 M lithium bis(trifluoromethanesulfonyl)imide (LiTFSI) dissolved in 1,3-dioxolane (DOL) and dimethoxy ethane (DME) with a volume ratio of 1:1 (Sigma Aldrich). All cells were assembled in an Ar glovebox starting from the negative case and crimped at 1200 psi using a MTI Corporation hydraulic crimping machine. Batteries were cycled on a Bio-Logic Variable Multichannel Potentiostat VMP3 in a voltage range of 1.0 V to 3.2 V (versus Li) with a rate of C/10 (where C/10 = Q/10 for one Li per CS molecular weight unit; specific current is 61 mA g^{-1}). Cyclic voltammetry was conducted between 1.0 V and 3.2 V with a scan rate of 0.1 mV s^{-1}. All electrochemical studies were performed at room temperature. Specific capacities are reported per gram of active disulfide material. Coulombic efficiency is reported as charge capacity divided by discharge capacity in per cent form.

^{1}H nuclear magnetic resonance (NMR) spectra were recorded on a AVANCE500 Bruker 500 MHz (11.7T) narrow bore spectrometer. ^{13}C and ^{7}Li solid state NMR with magic angle spinning (MAS) at 16k Hz was measured using a Bruker AVANCE III Ultrashield Plus 800 MHz (18.8T) narrow bore spectrometer. A Horiba Jobin–Yvon Lab ARAMIS instrument was used to measure Raman spectra with a 633 nm laser equipped with a confocal microscope and a 50× objective lens. Measurements were done using 500 μm aperture, 500 μm slit, and 600 gratings per mm, with exposure time of 1 s, averaged 10 times. Spectra of cast material was prepared by sealing a glass coverslip over the electrode such that it would remain air-free. X-ray photoelectron spectroscopy (XPS) was conducted using a Kratos Axis Ultra instrument loaded through an air-free transfer chamber with a monochromatic Al Kα source at 14.87 keV. Photoelectrons at pass energies of 20 eV and 80 eV were detected with a multichannel detector. The spectra were fit by the least-squares method to Voigt functions with Shirley baselines using CasaXPS.

Acknowledgements

We thank Dr. Jerry Hu for assistance with NMR experiments, and Dr. Megan Butala and Dr. Vicky Doan-Nguyen for helpful discussions on electrochemistry. Use of the Shared Experimental Facilities of the Materials Research Science and Engineering Center at UCSB (MRSEC NSF DMR 1720256) is gratefully acknowledged. The UCSB MRSEC is a member of the NSF-supported Materials Research Facilities Network (www.mrfn.org). M.B.P. acknowledges support from the Southern California Electrochemical Energy Storage Alliance (SCEESA), hosted by the UCSB California Nano-Systems Institute. We thank Toyal for the carbon coated aluminum used as the positive electrode current collector.

Conflict of interest

The authors declare no conflict of interest.

Keywords: battery · cathode · disulfide · lithium-sulfur battery

How to cite: *Angew. Chem. Int. Ed.* **2017**, *56*, 15118–15122
Angew. Chem. **2017**, *129*, 15314–15318

[1] A. Manthiram, Y. Fu, S. H. Chung, C. Zu, Y. S. Su, *Chem. Rev.* **2014**, *114*, 11751–11787.
[2] D. Larcher, J. Tarascon, *Nat. Chem.* **2014**, *7*, 19–29.
[3] *CRC Handbook of Chemistry and Physics* (Ed.: W. M. Haynes), CRC, Boca Raton, FL, **2013**.
[4] S. Cheon, K. Ko, J. Cho, S. Kim, E. Chin, *J. Electrochem. Soc.* **2003**, *150*, A796–A799.
[5] J. Nelson, S. Misra, Y. Yang, A. Jackson, Y. Liu, H. Wang, H. Dai, J. C. Andrews, Y. Cui, M. F. Toney, *J. Am. Chem. Soc.* **2012**, *134*, 6337–6343.
[6] Y.-X. Yin, S. Xin, Y.-G. Guo, L.-J. Wan, *Angew. Chem. Int. Ed.* **2013**, *52*, 13186–13200; *Angew. Chem.* **2013**, *125*, 13426–13441.
[7] R. D. Rauh, F. S. Shuker, J. M. Marston, S. B. Brummer, *J. Inorg. Nucl. Chem.* **1977**, *39*, 1761–1766.
[8] K. A. See, M. Leskes, J. M. Griffin, S. Britto, P. D. Matthews, A. Emly, A. Van der Ven, D. S. Wright, A. J. Morris, C. P. Grey, R. Seshadri, *J. Am. Chem. Soc.* **2014**, *136*, 16368–16377.
[9] Y. V. Mikhaylik, J. R. Akridge, *J. Electrochem. Soc.* **2004**, *151*, A1969–A1976.
[10] D. Moy, A. Manivannan, S. R. Narayanan, *J. Electrochem. Soc.* **2015**, *162*, 1–7.
[11] X. Ji, K. T. Lee, L. F. Nazar, *Nat. Mater.* **2009**, *8*, 500–506.
[12] Q. Sun, X. Fang, W. Weng, J. Deng, P. Chen, J. Ren, G. Guan, M. Wang, H. Peng, *Angew. Chem. Int. Ed.* **2015**, *54*, 10539–10544; *Angew. Chem.* **2015**, *127*, 10685–10690.
[13] S. Dörfler, M. Hagen, H. Althues, J. Tübke, S. Kaskel, M. J. Hoffmann, *Chem. Commun.* **2012**, *48*, 4097–4099.
[14] Y. Yang, G. Zheng, Y. Cui, *Chem. Soc. Rev.* **2013**, *42*, 3018–3032.
[15] X. Ji, S. Evers, R. Black, L. F. Nazar, *Nat. Commun.* **2011**, *2*, 325.
[16] S. Chung, A. Manthiram, *Adv. Mater.* **2014**, *26*, 1360–1365.
[17] C. Nan, Z. Lin, H. Liao, M. Song, Y. Li, E. J. Cairns, *J. Am. Chem. Soc.* **2014**, *136*, 4659–4663.
[18] G. Zheng, Y. Yang, J. J. Cha, S. S. Hong, Y. Cui, *Nano Lett.* **2011**, *11*, 4462–4467.
[19] H. Wang, Y. Yang, Y. Liang, J. T. Robinson, Y. Li, A. Jackson, Y. Cui, H. Dai, *Nano Lett.* **2011**, *11*, 2644–2647.
[20] Z. Li, J. Zhang, X. Wen, D. Lou, *Angew. Chem. Int. Ed.* **2015**, *54*, 12886–12890; *Angew. Chem.* **2015**, *127*, 13078–13082.

[21] N. Jayaprakash, J. Shen, S. S. Moganty, A. Corona, L. A. Archer, *Angew. Chem. Int. Ed.* **2011**, *50*, 5904 – 5908; *Angew. Chem.* **2011**, *123*, 6026 – 6030.
[22] L. Xiao, Y. Cao, J. Xiao, B. Schwenzer, M. H. Engelhard, L. V. Saraf, Z. Nie, G. J. Exarhos, J. Liu, *Adv. Mater.* **2012**, *24*, 1176 – 1181.
[23] H. Wang, W. Zhang, H. Liu, Z. Guo, *Angew. Chem. Int. Ed.* **2016**, *55*, 3992 – 3996; *Angew. Chem.* **2016**, *128*, 4060 – 4064.
[24] H. Wang, Y. Liu, M. Li, H. Huang, H. M. Xu, R. J. Hong, H. Shen, *Optoelectron. Adv. Mater., Rapid Commun.* **2010**, *4*, 1166 – 1169.
[25] J. Song, M. L. Gordin, T. Xu, S. Chen, Z. Yu, H. Sohn, J. Lu, Y. Ren, Y. Duan, D. Wang, *Angew. Chem. Int. Ed.* **2015**, *54*, 4325 – 4329; *Angew. Chem.* **2015**, *127*, 4399 – 4403.
[26] K. A. See, Y. S. Jun, J. A. Gerbec, J. K. Sprafke, F. Wudl, G. D. Stucky, R. Seshadri, *ACS Appl. Mater. Interfaces* **2014**, *6*, 10908 – 10916.
[27] C. Lee, Q. Pang, S. Ha, L. Cheng, S. Han, *ASC Cent. Sci.* **2017**, *3*, 605 – 613.
[28] L. Cheng, L. A. Curtiss, K. R. Zavadil, A. A. Gewirth, Y. Shao, K. G. Gallagher, *ACS Energy Lett.* **2016**, *1*, 503 – 509.
[29] H.-L. Wu, M. Shin, Y.-M. Liu, K. A. See, A. A. Gewirth, *Nano Energy* **2017**, *32*, 50 – 58.
[30] K. A. See, H.-L. Wu, K. C. Lau, M. Shin, L. Cheng, M. Balasubramanian, K. G. Gallagher, L. A. Curtiss, A. A. Gewirth, *ACS Appl. Mater. Interfaces* **2016**, *8*, 34360 – 34371.
[31] P. G. Bruce, B. Scrosati, J.-M. Tarascon, *Angew. Chem. Int. Ed.* **2008**, *47*, 2930 – 2946; *Angew. Chem.* **2008**, *120*, 2972 – 2989.
[32] N. S. Choi, Z. Chen, S. A. Freunberger, X. Ji, Y. K. Sun, K. Amine, G. Yushin, L. F. Nazar, J. Cho, P. G. Bruce, *Angew. Chem. Int. Ed.* **2012**, *51*, 9994 – 10024; *Angew. Chem.* **2012**, *124*, 10134 – 10166.
[33] H. Peng, Q. Zhang, *Angew. Chem. Int. Ed.* **2015**, *54*, 11018 – 11020; *Angew. Chem.* **2015**, *127*, 11170 – 11172.
[34] M. Liu, S. J. Visco, L. C. De Jonghe, *J. Electrochem. Soc.* **1989**, *136*, 2570 – 2575.
[35] S. J. Visco, C. C. Mailhe, L. C. De Jonghe, *J. Electrochem. Soc.* **1989**, *136*, 661.
[36] M. Liu, S. J. Visco, L. C. De Jonghe, *J. Electrochem. Soc.* **1991**, *138*, 1896 – 1901.
[37] J. A. Harnisch, R. J. Angelici, *Inorg. Chim. Acta* **2000**, *300 – 302*, 273 – 279.
[38] D. L. Turner, T. P. Vaid, P. W. Stephens, K. H. Stone, A. G. DiPasquale, A. L. Rheingold, *J. Am. Chem. Soc.* **2008**, *130*, 14 – 15.
[39] X. Huang, P. Sheng, Z. Tu, F. Zhang, J. Wang, H. Geng, Y. Zou, C. Di, Y. Yi, Y. Sun, W. Xu, D. Zhu, *Nat. Commun.* **2015**, *6*, 7408.
[40] H. E. van Wart, A. Lewis, H. A. Scheraga, F. D. Saevat, *Proc. Natl. Acad. Sci. USA* **1973**, *70*, 2619 – 2623.
[41] K. R. Ackermann, J. Koster, S. Schlücker, *Chem. Phys.* **2009**, *355*, 81 – 84.

Manuscript received: August 24, 2017
Accepted manuscript online: October 5, 2017
Version of record online: October 19, 2017

